DOI: 10.1002/anie.201004692

Liquid Crystals

Graphene Oxide Liquid Crystals**

*Ji Eun Kim, Tae Hee Han, Sun Hwa Lee, Ju Young Kim, Chi Won Ahn, Je Moon Yun, and Sang Ouk Kim**

Liquid crystal is the mesomorphic ordered state of anisotropic particles that bears liquid-like fluidity as well as crystal-like ordering.[1] Along with the recent enormous interest in carbon materials, carbon-based liquid crystals hold great promise for high-performance carbon material synthesis or device operation. Liquid-crystalline processing of carbon nanotubes, as well as mesophase pitch, has been employed for highly oriented carbon fiber spinning.[2] Discotic liquid crystals of synthetic graphitic hydrocarbons are promising components for advanced electronics and optoelectronics.[3] Herein, graphene oxide liquid crystals are introduced as a versatile new class of carbon-based liquid crystals.

Graphene oxide is the oxygenated form of a monolayer graphene platelet with strong mechanical properties, chemical functionalization capability, and extremely large surface area.[4] Graphene oxide is mass-producible from natural graphite by chemical oxidation and subsequent exfoliation.[5,6] The hydrophilic surface functional groups, such as epoxide, hydroxy, and carboxy groups that decorate the basal plane and the edge of graphene oxide enable monolayer exfoliation in common polar solvents including water.[7] The solution processibility of graphene oxide offers a practical route to carbon-based composites, paper, or thin film preparation.[6,8,9] Here, the liquid crystallinity of graphene oxide offers a versatile route to control the molecular organization and the corresponding properties of the carbon-based materials.[10–12]

We prepared exfoliated graphene oxide platelets by following a modified Hummer's method (see the Supporting Information). Graphite was obtained from three different commercial sources (Graphite A, Graphite B, and Graphite C—see the Supporting Information for more details). As presented in Figure 1 a, the prepared graphene oxide platelets revealed severe polydispersities in their shapes and sizes. The average size and size distribution, summarized in Table 1, varied significantly depending on the graphite source. The

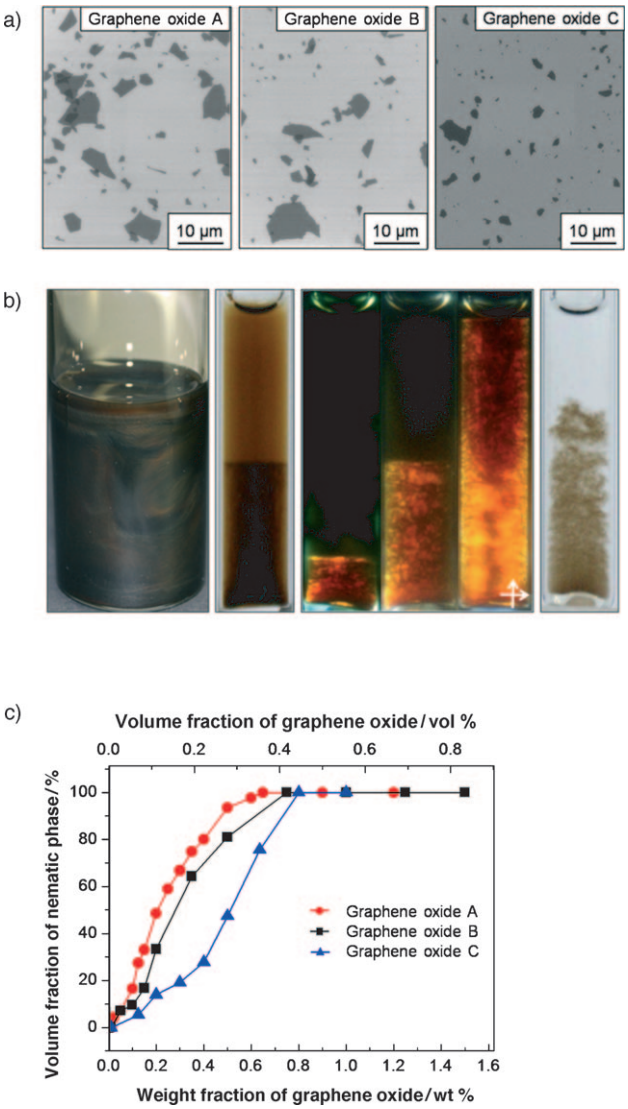

Figure 1. Graphene oxide liquid crystals from various graphite sources. a) Scanning electron microscopy (SEM) images of graphene oxide platelets exfoliated from various graphite sources. b) (Left to right) 0.5 wt% graphene oxide dispersion exhibiting a milky appearance; phase-separated 0.2 wt% dispersion three weeks after preparation; three phase-separated dispersions (0.05, 0.2, 0.5 wt%) located between crossed polarizers; coagulated 0.01 wt% dispersion upon adding 50 mM NaCl. c) Nematic phase volume fraction versus graphene oxide concentration.

[*] J. E. Kim, Dr. T. H. Han, Dr. S. H. Lee, J. Y. Kim, Dr. J. M. Yun, Prof. S. O. Kim
Department of Materials Science and Engineering
KI for the Nanocentury
Korea Advanced Institute of Science and Technology (KAIST)
305-701 Daejeon (Republic of Korea)
Fax: (+82) 42-350-3310
E-mail: sangouk.kim@kaist.ac.kr
Homepage: http://snml.kaist.ac.kr
Dr. C. W. Ahn
National Nanofab Center (NNFC)
305-806 Daejeon (Republic of Korea)

[**] This work was supported by the National Research Laboratory Program (R0A-2008-000-20057-0), Converging Research Center Program (2009-0093659), World Premier Materials (WPM) program (10037689), and Pioneer Research Center Program (2009-0093758), funded by the Korean government (MEST & MKE).

Supporting information for this article is available on the WWW under http://dx.doi.org/10.1002/anie.201004692.

Table 1: Mean diameter ($\langle D \rangle$), standard deviation of the diameter (σ_D), and mean aspect ratio of sheets of the graphene oxides A–C.

	$\langle D \rangle$	σ_D	Aspect ratio
Graphene oxide A	1.65	1.28	ca. 1600
Graphene oxide B	1.22	1.16	ca. 1200
Graphene oxide C	0.75	0.88	ca. 700

average aspect ratio of the graphene oxide platelets with atomic-scale thickness (ca. 1.0 nm) was over 700.

Graphene oxide aqueous dispersions were prepared by dispersing graphene oxide platelets in deionized water by mild sonication. Any acidic or ionic impurities in the dispersions were removed by dialysis, which is a crucial step for liquid-crystal formation (see Figure S1 in the Supporting Information). A limited amount of unexfoliated graphite oxide particles was carefully discarded by centrifugation (see Figure S2 in the Supporting Information). As such, the prepared graphene oxide dispersion exhibited an inhomogeneous, chocolate-milk-like appearance to the naked eye (Figure 1 b, left). This milky appearance can be mistaken for aggregation or precipitation of the graphene oxide but, in fact, it is a nematic liquid crystal.

A low-concentration dispersion (typically 0.05–0.6 wt %) immobilized for a sufficiently long time (usually more than 3 weeks) macroscopically phase-separated into two phases. While the low-density top phase was optically isotropic, the high-density bottom phase demonstrated prominent optical birefringence between two crossed polarizers. A typical nematic schlieren texture consisting of dark and bright brushes was observed in the bottom phase. This is biphasic behavior, where an isotropic phase and nematic phase coexist. The compositional range for the biphase was significantly broad because of the large polydispersity of the graphene oxide platelets.[13] We note that ionic strength and pH significantly influence the stability of graphene oxide liquid crystals.[4d] The electrostatic repulsion from the dissociated surface functional groups such as carboxylate plays a crucial role in the stability of graphene oxide liquid crystals. Thus, reducing repulsive interaction by increasing ionic strength or lowering pH increased the coagulation of graphene oxide platelets (Figure 1 b, right).

Figure 1 c presents the liquid-crystal phase transitions of various graphene oxides. The liquid crystallinity was observed for all graphite sources. Detailed chemical analysis revealed that the graphene oxides had a similar degree of oxidation regardless of the graphite sources (see Figure S3 and Table S1 in the Supporting Information). As plotted with red circles (Figure 1 c), the graphene oxide with the largest shape anisotropy (graphene oxide A) completed nematic phase formation at 0.53 wt %. In contrast, the biphasic range for the smallest shape anisotropy of graphene oxide (graphene oxide C) persisted up to 0.75 wt %. Above these critical concentrations, the nematic phases were maintained up to the water boiling temperature (see Figure S4 in the Supporting Information). We note that the observed transition concentrations are generally lower than the theoretical calculated values based on a polydisperse hard-disk model (see Table S2 in the Supporting Information).[13] Since pure water is a good solvent, graphene oxide platelets form stretched conformations.[14] Moreover, the electrostatic repulsion, caused by charged surface functional groups, and irregular shapes of graphene oxide platelets can swell the effective size of graphene oxide platelets and, thus, lower the transition concentrations.

Figure 2 a shows the optical microscopy image of a 0.3 wt % graphene oxide dispersion located between a pair of crossed polarizers. Schlieren texture was observed with disclinations of various signs and strengths.[1a–c] The birefringent optical texture reflects the local orientation of the graphene oxide platelets. The platelets oriented parallel to one of the crossed polarizer axes in the dark brushes but

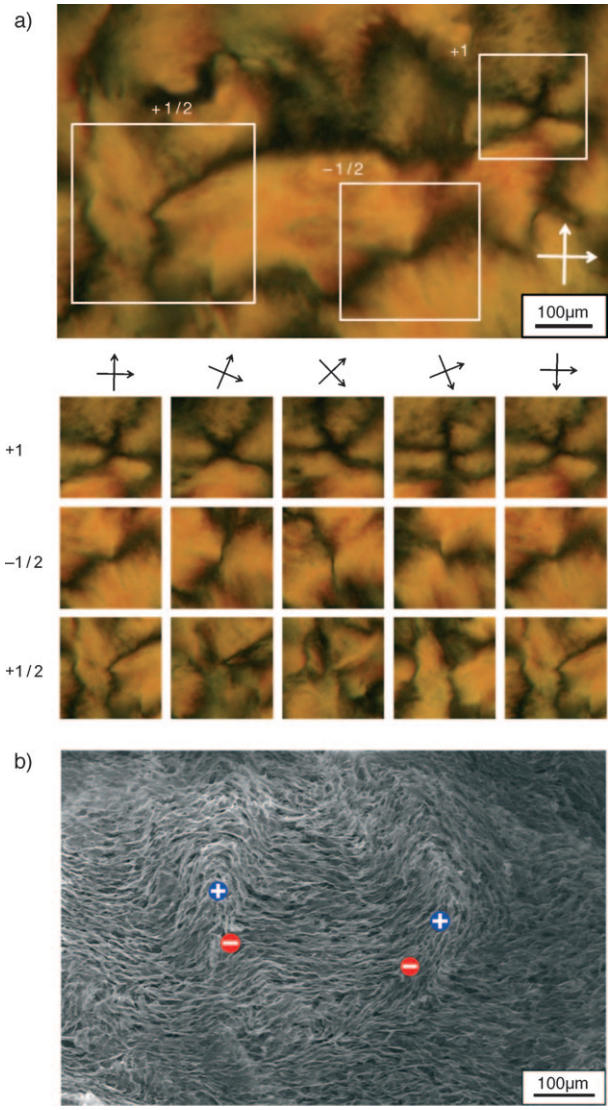

Figure 2. Disclination morphologies of graphene oxide liquid crystals. a) Typical nematic schlieren texture of a 0.3 wt% dispersion with $\pm^1/_2$ disclinations and a +1 disclination. Successive rotations of crossed polarizers accompanied the rotation of brushes at various rotating rates and directions. b) SEM image of a graphene oxide liquid crystal in a freeze-dried sample (0.5 wt%). Blue and red symbols indicate $+^1/_2$ and $-^1/_2$ disclinations, respectively.

oriented in an intermediate direction in the bright brushes. A pair of dark or bright brushes meets to constitute a $\pm 1/2$ disclination. Upon rotation of the crossed polarizers, the $\pm 1/2$ disclination morphology rotated at twice the angular velocity of the polarizers. The singular points where four dark or bright brushes meet are ± 1 disclinations. The four brushes of a ± 1 disclination rotated at the same angular velocity as the polarizers. The sign of disclination could be determined by the rotation direction of the brushes. The brushes of a positive disclination rotated in the same direction as the crossed polarizers, while those of a negative disclination rotated in the opposite direction. The birefringent texture of the graphene oxide liquid crystals exhibited a high density of $\pm 1/2$ disclinations, which is a typical feature of nematic liquid crystals.

The local orientation of the graphene oxide liquid crystals could be directly visualized by SEM after removing the aqueous medium. A concentrated liquid-crystalline dispersion (0.5 wt%) was quickly quenched in liquid nitrogen and subsequently freeze-dried to leave graphene oxide platelets as oriented in the nematic phase. The remaining cooperative orientation of graphene oxide sheets was consistent with the typical disclination morphology. Figure 2b shows a SEM image of the graphene oxide alignment around a few $\pm 1/2$ disclinations. Graphene oxide platelets are smoothly bent along the surrounding director orientation.[14] However, the local orientation shows discontinuity at the disclination cores, as generally observed in liquid-crystalline disclinations.

Macroscopic orientation of liquid crystals is readily tunable by an external field.[1a,b,f] However, an electric field, which is widely used in liquid-crystal-display switching, is inapplicable to graphene oxide liquid crystals. Under an electric field, the negatively charged graphene oxide platelet underwent electrophoretic migration toward the cathode. Afterwards, the graphene oxide accumulated at the cathode became electrochemically reduced (see Figure S5 in the Supporting Information). Instead of an electric field, a magnetic field or mechanical deformation successfully controlled the macroscopic alignment of graphene oxide liquid crystals.

Figure 3 presents the evolution of the birefringent texture of graphene oxide liquid crystals under a magnetic field. Thin sample preparation by squeezing left a shear-induced morphology (Figure 3a). After prolonged annealing at room temperature (ca. 3 h), the shear-induced morphology disappeared and a typical nematic schlieren texture evolved (Figure 3b). A strong magnetic field (H, 0.25 T) was applied to the schlieren textured sample, as illustrated in Figure 3c. The magnetic-field-induced alignment could be monitored (see Movie S1 in the Supporting Information). The domains with different liquid-crystal orientation, initially separated by disclinations, gradually reoriented and merged into a large domain (Figure 3c). Because of the weak magnetism of the bare graphene oxide platelets, complete alignment of the entire sample took more than several hours (typically 5 h).[12a] The magnetic alignment could be remarkably enhanced by decorating graphene oxide with magnetic nanoparticles. The graphene oxides functionalized with iron oxide (Fe_2O_3) nanoparticles maintained the liquid crystallinity in an aqueous medium and completed field-induced alignment within several seconds under the same strength of magnetic field (see Movie S2 and Figure S6 in the Supporting Information).[15]

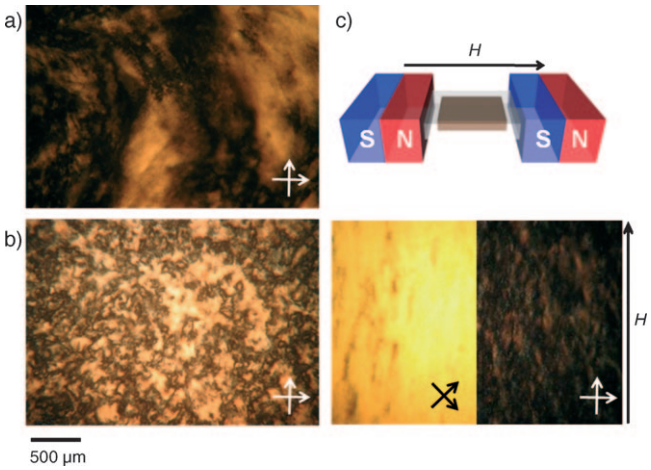

Figure 3. Magnetic-field-induced alignment of graphene oxide liquid crystals. a) Shear-induced birefringent morphology formed after sample preparation. b) Nematic schlieren morphology formed about 3 h after sample preparation without any external field. c) Top: experimental scheme for magnetic field application; bottom: magnetic-field-induced highly aligned liquid-crystal texture.

The liquid crystallinity of graphene oxide could also be maintained in a polymer matrix. We prepared poly(acrylic acid) (PAA)/graphene oxide nanocomposites and investigated their mechanical-deformation-induced alignment behavior. PAA, a widely used water-soluble polymer, was dissolved in an aqueous dispersion of graphene oxide (Figure 4a). The resultant three-component mixture (weight fraction of water/PAA/graphene oxide = 25.9:5:0.1) maintained a birefringent schlieren texture under crossed polarizers (Figure 4b). After sufficient evaporation of water, the remaining gel composites were uniaxially deformed by hand drawing. The hand-drawn fibers exhibited a strong optical birefringence (Figure 4c).[16] The cross-sectional SEM view along the fiber axis presents the graphene oxide platelets as highly aligned and stretched along the mechanical drawing direction. In the radial cross-sectional view, domains of collectively oriented graphene oxide platelets were observed (Figure 4e).

In summary, we have demonstrated the liquid crystallinity of graphene oxide aqueous dispersions. Despite the tremendous research interest in graphene oxide, its liquid crystallinity has first been demonstrated here. The liquid crystallinity could be maintained upon the decoration of the graphene oxide platelets with nanoparticles or by including an additional polymer component in the solvent medium. This may significantly broaden the material composition and functionality of graphene oxide liquid crystals. Moreover, the orientation of graphene oxide liquid crystals could be manipulated by a magnetic field or mechanical deformation. Such versatility of graphene oxide liquid crystals along with their mass producibility from naturally abundant graphite offers a viable route to high-performance nanocomposites,

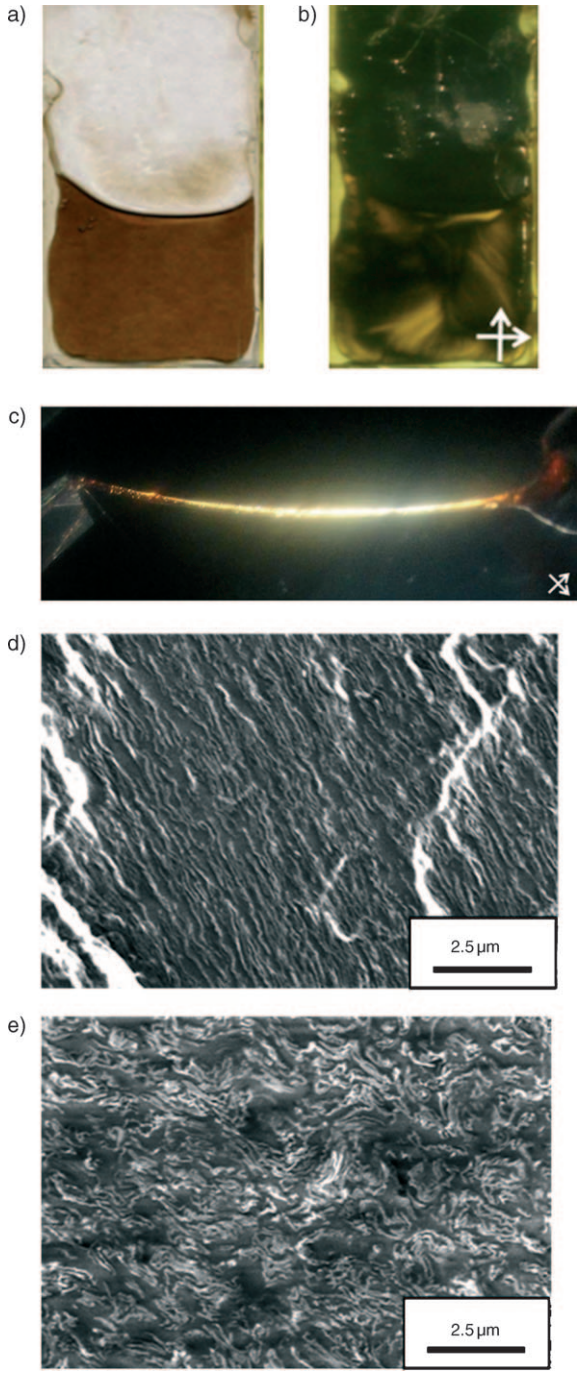

Figure 4. Mechanical-deformation-induced alignment of PAA/graphene oxide composites. Water/PAA/graphene oxide three-component liquid-crystal mixtures: a) without and b) with crossed polarizers. c) Hand-drawn gel composite fiber. The strong optical birefringence was caused by homogeneously dispersed, uniaxially oriented graphene oxide platelets. d) Highly aligned graphene oxide morphology along the fiber axis. e) Randomly oriented graphene oxide morphology in the fiber cross section.

optical materials, energy-storage materials, and many other applications.[4h,9,17]

Received: July 29, 2011
Revised: October 10, 2011
Published online: February 23, 2011

Keywords: dispersions · graphene · liquid crystals · phase transitions · polarized spectroscopy

[1] a) P. G. de Gennes, J. Prost in *The Physics of Liquid Crystals*, Oxford University Press, Oxford, **1993**; b) S. Chandrasekhar in *Liquid Crystals*, Cambridge University Press, Cambridge, **1992**; c) A. M. Donald, A. H. Windle, S. Hanna in *Liquid Crystalline Polymers*, Cambridge University Press, Cambridge, **2006**; d) F. M. van der Kooij, K. Kassapidou, H. N. W. Lekkerkerker, *Nature* **2000**, *406*, 868–871; e) S.-W. Lee, C. Mao, C. E. Flynn, A. M. Belcher, *Science* **2002**, *296*, 892–895; f) T. H. Han, J. Kim, J. S. Park, C. B. Park, H. Ihee, S. O. Kim, *Adv. Mater.* **2007**, *19*, 3924–3927; g) L.-S. Li, J. Walda, L. Manna, A. P. Alivisatos, *Nano Lett.* **2002**, *2*, 557–560; h) M. Nakata, G. Zanchetta, B. D. Chapman, C. D. Jones, J. O. Cross, R. Pindak, T. Bellini, N. A. Clark, *Science* **2007**, *318*, 1276–1279.

[2] a) W. Song, I. A. Kinloch, A. H. Windle, *Science* **2003**, *302*, 1363; b) V. A. Davis, A. N. G. Parra-Vasquez, M. J. Green, P. K. Rai, N. Behabtu, V. Prieto, R. D. Booker, J. Schmidt, E. Kesselman, W. Zhou, H. Fan, W. W. Adams, R. H. Hauge, J. E. Fischer, Y. Cohen, Y. Talmon, R. E. Smalley, M. Pasquali, *Nat. Nanotechnol.* **2009**, *4*, 830–834; c) K. Jian, H.-S. Shim, A. Schwartzman, G. P. Crawford, R. H. Hurt, *Adv. Mater.* **2003**, *15*, 164–167.

[3] a) L. Schmidt-Mende, A. Fechtenkötter, K. Müllen, E. Moons, R. H. Friend, J. D. MacKenzie, *Science* **2001**, *293*, 1119–1122; b) J. Wu, W. Pisula, K. Müllen, *Chem. Rev.* **2007**, *107*, 718–747.

[4] a) D. A. Dikin, S. Stankovich, E. J. Zimney, R. D. Piner, G. H. B. Dommett, G. Evmenenko, S. T. Nguyen, R. S. Ruoff, *Nature* **2007**, *448*, 457–460; b) A. K. Geim, *Science* **2009**, *324*, 1530–1534; c) C. Gómez-Navarro, M. Burghard, K. Kern, *Nano Lett.* **2008**, *8*, 2045–2049; d) D. Li, M. B. Müller, S. Gilje, R. B. Kaner, G. G. Wallace, *Nat. Nanotechnol.* **2008**, *3*, 101–105; e) D. R. Dreyer, S. Park, C. W. Bielawski, R. S. Ruoff, *Chem. Soc. Rev.* **2010**, *39*, 228–240; f) Y. Zhu, S. Murali, W. Cai, X. Li, J. W. Suk, J. R. Potts, R. S. Ruoff, *Adv. Mater.* **2010**, *22*, 3906–3924; g) M. Segal, *Nat. Nanotechnol.* **2009**, *4*, 612–614; h) S. H. Lee, D. H. Lee, W. J. Lee, S. O. Kim, *Adv. Funct. Mater.* **2011**, DOI: 10.1002/adfm.201002048.

[5] a) B. C. Brodie, *Ann. Chim. Phys.* **1860**, *59*, 466; b) W. S. Hummers, R. E. Offeman, *J. Am. Chem. Soc.* **1958**, *80*, 1339.

[6] S. Stankovich, D. A. Dikin, G. H. B. Dommett, K. M. Kohlhaas, E. J. Zimney, E. A. Stach, R. D. Piner, S. T. Nguyen, R. S. Ruoff, *Nature* **2006**, *442*, 282–286.

[7] W. Cai, R. D. Piner, F. J. Stadermann, S. Park, M. A. Shaibat, Y. Ishii, D. Yang, A. Velamakanni, S. J. An, M. Stoller, J. An, D. Chen, R. S. Ruoff, *Science* **2008**, *321*, 1815–1817.

[8] a) Y. Hernandez, V. Nicolosi, M. Lotya, F. M. Blighe, Z. Sun, S. De, I. T. Mcgovern, B. Holland, M. Byrne, Y. K. Gunko, J. J. Boland, P. Niraj, G. Duesberg, S. Krishnamurthy, R. Goodhue, J. Hutchison, V. Scardaci, A. C. Ferrari, J. N. Coleman, *Nat. Nanotechnol.* **2008**, *3*, 563–568; b) V. C. Tung, M. J. Allen, Y. Yang, R. B. Kaner, *Nat. Nanotechnol.* **2009**, *4*, 25–29; c) G. Eda, G. Fanchini, M. Chhowalla, *Nat. Nanotechnol.* **2008**, *3*, 270–274.

[9] a) S. H. Lee, D. R. Dreyer, J. An, A. Velamakanni, R. D. Piner, S. Park, Y. Zhu, S. O. Kim, C. W. Bielawski, R. S. Ruoff, *Macromol. Rapid Commun.* **2010**, *31*, 281–288; b) S. H. Lee, J. S. Park, B. K. Lim, C. B. Mo, W. J. Lee, J. M. Lee, S. H. Hong, S. O. Kim, *Soft Matter* **2009**, *5*, 2343–2346; c) D. H. Lee, J. E. Kim, T. H. Han, J. W. Hwang, S. Jeon, S.-Y. Choi, S. H. Hong, W. J. Lee, R. S. Ruoff, S. O. Kim, *Adv. Mater.* **2010**, *22*, 1247–1252; d) T. H. Han, W. J. Lee, D. H. Lee, J. E. Kim, E.-Y. Choi, S. O. Kim, *Adv. Mater.* **2010**, *22*, 2060–2064; e) B. H. Kim, J. Y. Kim, S.-J. Jeong, J. O. Hwang, D. H. Lee, D. O. Shin, S.-Y. Choi, S. O. Kim, *ACS Nano* **2010**, *4*, 5464–5470; f) E.-Y. Choi, T. H. Han, J. Hong, J. E. Kim, S. H. Lee, H. W. Kim, S. O. Kim, *J. Mater. Chem.* **2010**, *20*, 1907–1912; g) S. H. Lee, H. W. Kim, J. O.

Hwang, W. J. Lee, J. Kwon, C. W. Bielawski, R. S. Ruoff, S. O. Kim, *Angew. Chem.* **2011**, *122*, 10282 – 10286; *Angew. Chem. Int. Ed.* **2011**, *49*, 10084 – 10088.
[10] S. Park, R. S. Ruoff, *Nat. Nanotechnol.* **2009**, *4*, 217 – 224.
[11] a) K. S. Novoselov, A. K. Geim, S. V. Morozov, D. Jiang, Y. Zhang, S. V. Dubonos, I. V. Grigorieva, A. A. Firsov, *Science* **2004**, *306*, 666 – 669; b) F. Schedin, A. K. Geim, S. V. Morozov, E. W. Hill, P. Blake, M. I. Katsnelson, K. S. Novoselov, *Nat. Mater.* **2007**, *6*, 652 – 655; c) M. D. Stoller, S. Park, Y. Zhu, J. An, R. S. Ruoff, *Nano Lett.* **2008**, *8*, 3498 – 3502.
[12] a) Y. Wang, Y. Huang, Y. Song, X. Zhang, Y. Ma, J. Liang, Y. Chen, *Nano Lett.* **2009**, *9*, 220 – 224; b) G. Eda, Y.-Y. Lin, C. Mattevi, H. Yamaguchi, H.-A. Chen, I.-S. Chen, C.-W. Chen, M. Chhowalla, *Adv. Mater.* **2010**, *22*, 505 – 509; c) C.-H. Lu, H.-H. Yang, C.-L. Zhu, X. Chen, G.-N. Chen, *Angew. Chem.* **2009**, *121*, 4879 – 4881; *Angew. Chem. Int. Ed.* **2009**, *48*, 4785 – 4787; d) Z. Wei, D. Wang, S. Kim, S.-Y. Kim, Y. Hu, M. K. Yakes, A. R. Laracuente, Z. Dai, S. R. Marder, C. Berger, W. P. King, W. A. de Heer, P. E. Sheehan, E. Riedo, *Science* **2010**, *328*, 1373 – 1376.
[13] a) F. M. van der Kooij, H. N. W. Lekkerkerker, *J. Phys. Chem. B* **1998**, *102*, 7829 – 7832; b) M. A. Bates, D. Frenkel, *J. Chem. Phys.* **1999**, *110*, 6553 – 6559.
[14] M. S. Spector, E. Naranjo, S. Chiruvolu, J. A. Zasadzinski, *Phys. Rev. Lett.* **1994**, *73*, 2867 – 2870.
[15] M. Mikhaylova, D. K. Kim, C. C. Berry, A. Zagorodni, M. Toprak, A. S. G. Curtis, M. Muhammed, *Chem. Mater.* **2004**, *16*, 2344 – 2354.
[16] a) C. M. Koo, H. T. Ham, S. O. Kim, K. H. Wang, I. J. Chung, D. C. Kim, W. C. Zin, *Macromolecules* **2002**, *35*, 5116 – 51222; b) C. M. Koo, S. O. Kim, I. J. Chung, *Macromolecules* **2003**, *36*, 2748 – 2757.
[17] a) D. H. Lee, J. A. Lee, W. J. Lee, S. O. Kim, *Small* **2011**, *7*, 95 – 100; b) J. M. Lee, J. S. Park, S. H. Lee, H. Kim, S. Yoo, S. O. Kim, *Adv. Mater.* **2011**, *23*, 629 – 633.

